

A Glucose/O₂ Biofuel Cell Based on Graphene and Multiwalled Carbon Nanotube Composite Modified Electrode

Balamurugan Devadas, Veerappan Mani, Shen-Ming Chen*

Department of Chemical Engineering and Biotechnology, National Taipei University of Technology, No.1, Section 3, Chung-Hsiao East Road, Taipei 106, Taiwan (R.O.C).

*E-mail: smchen78@ms15.hinet.net

Received: 17 July 2012 / Accepted: 8 August 2012 / Published: 1 September 2012

We have constructed a glucose/O₂ biofuel cell (BFC) with electrochemically reduced graphene oxide - multiwalled carbon nanotube (ERGO-MWCNT) modified glassy carbon electrode (GCE) as anode and graphene-Pt composite modified GCE as cathode. The electrochemical characterization results show that enzyme GOx was well immobilized onto the composite modified electrode. Moreover the composite modified film exhibits excellent catalytic ability towards the oxidation of glucose in the presence of redox mediator hydroquinone (HQ). Graphene -Pt composite has been prepared by simple sodium borohydride reduction method and characterized. The graphene-Pt composite modified GCE shows good electrocatalytic activity towards O₂ reduction. A membraneless glucose/O₂ biofuel cell (BFC) has been developed by employing ERGO-MWCNT modified GCE as anode and graphene-Pt as cathode. The maximum power density of 46 $\mu\text{W cm}^{-2}$ was achieved for the constructed biofuel. The results showed that graphene based composites are potential candidates for the development of efficient biofuel cells.

Keywords: ERGO-MWCNT, hydroquinone, cathode, O₂ reduction, biofuel cell.

1. INTRODUCTION

Biofuel cells (BFCs) are special kind of fuel cells, employing enzymes as the biocatalyst for the conversion of chemical energy into electrical energy [1]. Although, BFCs have been known for long time [2], they catch enormous attention only in the recent years and are expected to be one of the promising next generation green energy devices. BFCs have numerous applications in the fields such as implantable devices [3], waste water treatment [4], drug delivery [5] and biosensors [6]. The important advantageous of BFCs over other conventional fuel cells are selectivity of the enzyme

towards fuel and highly feasible working conditions such as physiological pH and ambient temperature [7]. Besides, the fuels for BFCs are from renewable energy sources usually sugars or organic acids and most often glucose [8]. However, BFCs also have certain drawbacks such as poor stability because of the short lifetime of enzyme and low power densities [7]. Electrons can be transferred between the electrode and the active site either with the aid of mediators (Mediated electron transfer) or without any mediators (Direct electron transfer) [9]. Since the redox centre of the enzyme is deeply buried into the protein chains, generally mediators are adopted to shuttle the electrons between the enzymes and electrodes which eventually enhances the efficiency and power density of the BFCs [10, 11]. Among different kinds of BFCs, glucose/O₂ biofuel cell is the most studied, where glucose oxidation occurs at the anode and oxygen reduction occurs at the cathode [12, 13].

Owing to its unique structural and electronic properties, carbon nanotubes (CNTs) find outstanding applications in various research areas [14-16]. Until now, numerous enzymatic BFCs were developed based on CNTs modified electrode. L. Mao et al. developed a glucose/O₂ BFC based on single walled carbon nanotube (SWNT) with glucose dehydrogenase (GDH) as the anode biocatalyst with NAD⁺ as the cofactor and laccase as the cathode biocatalyst [17]. S. Dong et al. demonstrated a BFC using multiwalled carbon nanotubes (MWCNT) - ionic liquid gel modified graphite electrodes as the matrix [18]. Z. Iqbal et al. reported a Membrane-less and mediator-free direct electron transfer enzymatic BFCs with bioelectrodes comprised of single wall carbon nanotubes (SWNTs) deposited on porous silicon (pSi) substrates [19].

Recently, graphene 2D carbon material composed of a monolayer of sp² bonded carbon atoms has attracted great attention and emerged as a promising material, due to its interesting physicochemical properties [20-23]. In the recent years, several strategies have been employed for the exploitation of graphene material based modified electrodes towards biofuel cell applications. W. Zheng et al. constructed a nanographene platelets (NGPs)-based glucose/O₂ biofuel cell (BFC) with glucose oxidase (GOx) as the anode and the laccase as the cathode [24]. C. Liu et al. developed a miniaturized membraneless glucose/O₂ biofuel cell based on the surface engineering of graphene-GOx composite [25]. C.Z. Li et al. employed silica sol-gel immobilized graphene sheets composite as a matrix for the immobilization of enzymes in both anode and cathode platform and successfully developed a membraneless BFC [26].

Herein, we use a simple and efficient approach to harvest the excellent electrochemical properties of both MWCNT and graphene by combining them via non-covalent π - π stacking interactions. We utilize graphene oxide (GO), an oxygenated derivative of graphene as a precursor to prepare graphene oxide - MWCNT composite by simple sonication approach [27, 28]. Afterwards, the composite was electrochemically reduced and employed for GOx immobilization [29]. Further, we prepared graphene - Pt composite by simple sodium borohydride reduction and employed as a cathode material [30]. At last, we successfully constructed a BFC with ERGO-MWCNT/GOx/Nf modified GCE as anode for the oxidation of glucose and Graphene/Pt modified GCE as cathode for the O₂ reduction [scheme 1].

2. EXPERIMENTAL

2.1 Reagents

MWCNT (bundled > 95%, O.D \times I.D \times length of 7-15 nm \times 3-6 nm \times 0.5-200 μ m), graphite (powder, <20 μ m) and GOx (type x-s from aspergillus Niger) were purchased from sigma-Aldrich and used as received. 5 wt% nafion (Nf) was purchased from Aldrich and the required Nf concentrations were prepared using 95% pure ethanol. The mediator hydroquinone (HQ) was purchased from Alfa Aesar. All the reagents used were of analytical grade and used without purification. The supporting electrolyte used for electrochemical studies was 0.1 M Phosphate buffer solution (PBS), prepared using Na₂HPO₄ and NaH₂PO₄ and the pH was adjusted either using H₂SO₄ or NaOH.

2.2 Apparatus

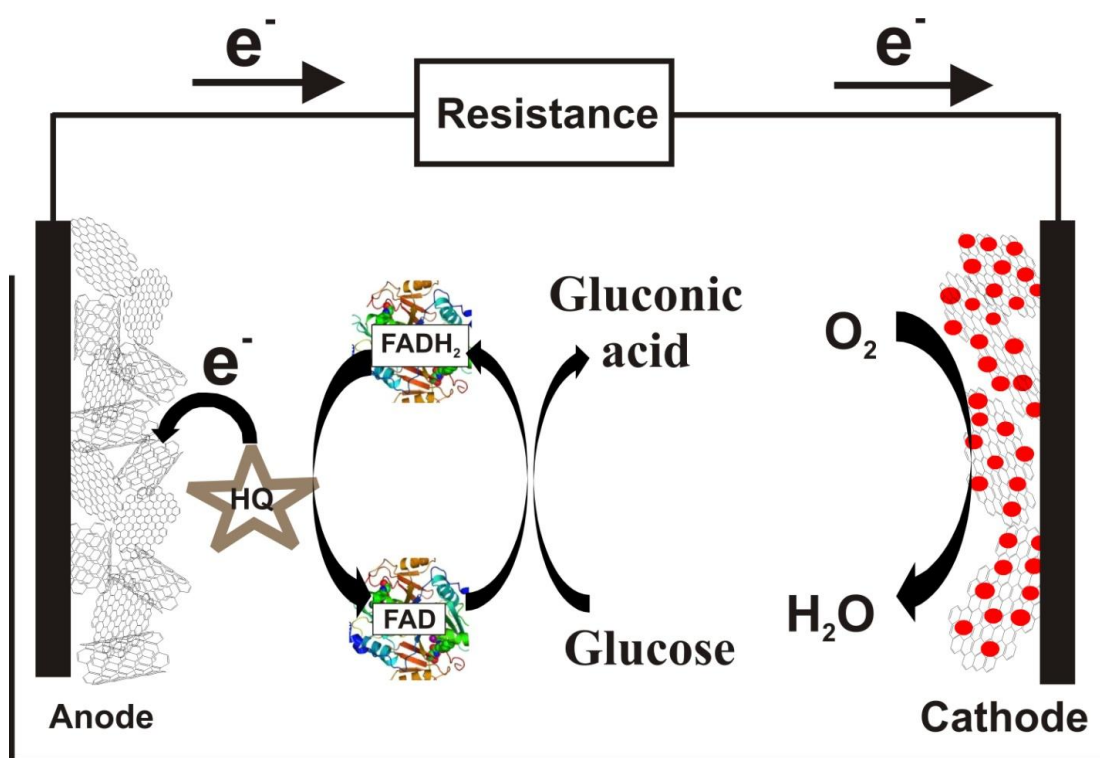
The electrochemical measurements were carried out using CHI 611a work station with a conventional three electrode cell using BAS GCE as working electrode (area 0.07 cm²), Ag|AgCl (sat. KCl) as reference electrode and Pt wire as counter electrode. Amperometric measurements were performed with analytical rotator AFMSRX (PINE instruments, USA) with a rotating disc electrode (RDE) having working area of 0.24 cm². Glucose solution was kept aside for one day to achieve mutarotation. Prior to each experiment, all the solutions were deoxygenated by purging pre-purified N₂ gas for 15 min unless otherwise specified. Surface morphological studies were carried out using Hitachi S-3000 H scanning electron microscope (SEM). Energy dispersive X-ray (EDX) spectra was recorded using HORIBA EMAX X-ACT (Sensor + 24V=16 W, resolution at 5.9 keV).

2.3 Fabrication of Anode

Graphite oxide was prepared by modified Hummer's method [31] and it was dispersed in water. The as-prepared graphite oxide was exfoliated through ultrasonication for 2 h. Then, it was centrifuged for 30 min at 4000 rpm and the yellowish brown supernatant containing GO platelets were separated and used for the composite preparation. Then 5 mg of MWCNT was added into 10 ml of aqueous GO solution (0.5 mg mL⁻¹) and the resulting mixture was subjected to ultrasonication for 2 h. Two consecutive centrifugation cycles (30 min each) at 8000 and 14000 RPM have been performed to remove the excess amount of MWCNT and GO [27]. Thus obtained GO-MWCNT was washed with water, overnight dried and redispersed in water at the concentration of 0.5 mg mL⁻¹. For comparative study, pristine GO and MWCNT dispersions were also prepared in water and DMF solvents respectively.

GCE surface was polished well with 0.05 μ m alumina slurry using a Buehler polishing kit, then washed with water, ultrasonicated and dried. 5 μ l of GO-MWCNT dispersion was drop casted onto the pre-cleaned GCE and dried at room temperature for 20 min. The composite film modified GCE was gently washed with water and transferred to an electrochemical cell containing 0.1 M PBS (pH 5). It was electrochemically reduced by performing 3 successive cyclic voltammograms in the potential

range of 0 to -1.5 V [29]. As evident from the Fig.1A, a large cathodic peak was appeared at -1.1 V corresponding to the electrochemical reduction of oxygen functionalities of GO. The onset potential (-0.3) was comparatively lower than that of pristine GO (-0.75 V), indicating considerable promotion of GO reduction after incorporating with MWCNT [20]. The electrochemically reduced GO-MWCNT (ERGO-MWCNT) composite film modified GCE was washed with water and dried. After that 6 μl (10 mg mL^{-1}) of GOx was evenly distributed on the composite modified GCE and dried at ambient conditions. Finally 2 μl (0.5%) of Nf was drop casted onto the surface of modified electrode to avoid the GOx leaching. Thus obtained ERGO-MWCNT/GOx/Nf composite film modified GCE was rinsed with water and stored in PBS when not in use.



Scheme 1. Schematic representation of the assembled biofuel cell with ERGO-MWCNT/GOx/Nf as bioanode and GCE/Graphene-Pt composite as biocathode.

2.4 Fabrication of cathode

GO (0.2mg/ml) was mixed with 3 ml of 0.02M K_2PtCl_6 solution, stirred for 20 minutes and the pH value of the resulting mixture was adjusted to 10 using 1 M NaOH solution [30]. Then, 400mg of NaBH_4 was slowly added and the reaction mixture was kept stirred for 20 hr. Upon completion of the reaction, the final reaction mixture was washed successively with ethanol and water. Further the obtained Graphene – Pt composite was dried overnight and redispersed (0.5 mg mL^{-1}) in 0.5% nafion. Then 5 μl of as prepared Graphene – Pt composite was drop casted onto the pre-cleaned GCE surface and dried. Further GCE/Graphene-Pt modified electrode was rinsed with water and stored in PBS when not in use.

3. RESULTS AND DISCUSSION

3.1. SEM and EDX Characterization of anode

Fig. 1 shows the SEM images of ERGO-MWCNT (B), ERGO-MWCNT/GOx (C) and ERGO-MWCNT/GOx/Nf (D) modified electrodes.

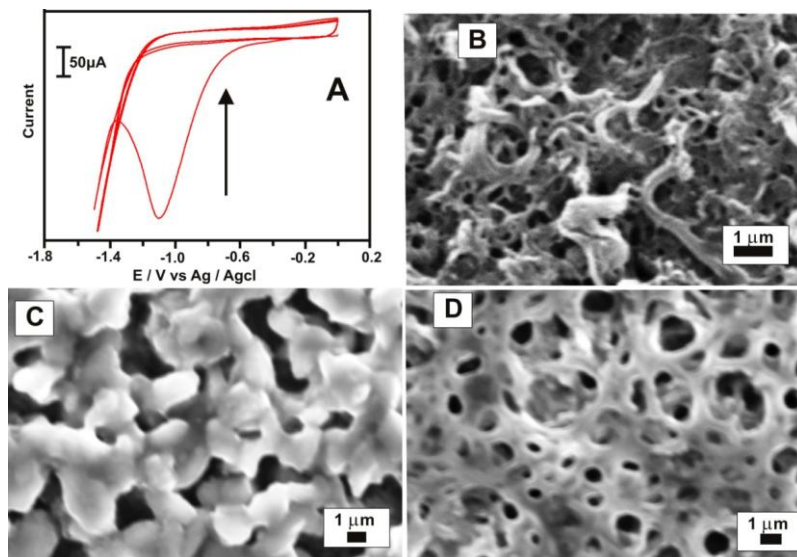


Figure 1. (A) Electrochemical reduction of GO-MWCNT composite for 3 cycles in N_2 saturated PBS (pH 5) at the Scan rate of 50 mVs^{-1} . SEM images of ERGO-MWCNT (B), ERGO-MWCNT/GOx (C) and ERGO-MWCNT/GOx/Nf (D).

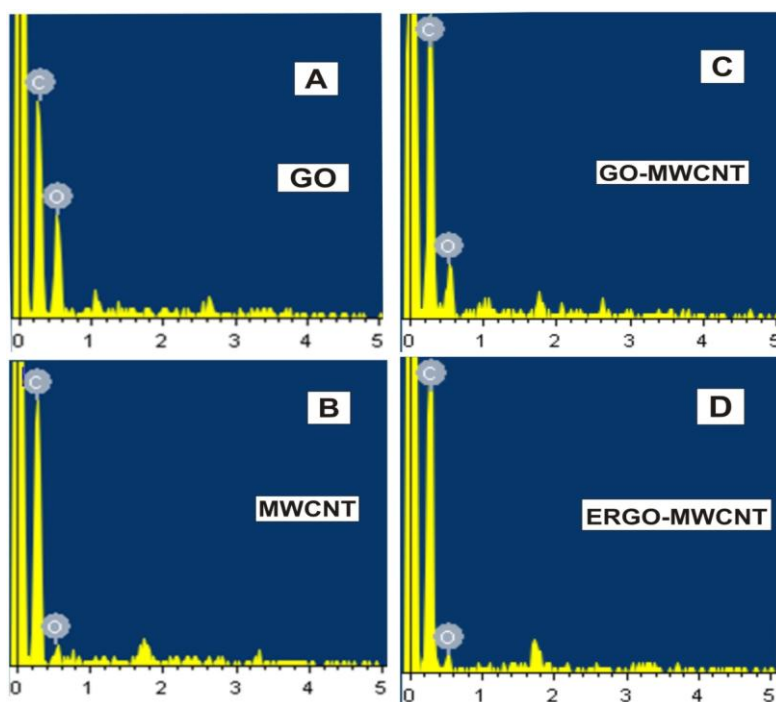


Figure 2. EDX spectra of GO (A), MWCNT (B), GO-MWCNT (C) and ERGO-MWCNT (D).

SEM image of ERGO-MWCNT composite clearly indicating that tubular network of MWCNT were firmly attached with graphene sheets. After GOx incorporated into the film, the morphology becomes totally different from that of only composite. The SEM image ERGO-MWCNT/GOx seems to be GOx molecules were uniformly distributed on the surface of the ERGO-MWCNT modified film.

This clogged morphology of GOx showed that more amount of GOx molecules were immobilized onto the ERGO-MWCNT surface. High GOx coverage has been achieved owing to the good affinity of the composite towards GOx. Further, the SEM image of ERGO-MWCNT/GOx/Nf modified film shows the characteristic nafion morphology along with small cavities, resulting because of solvent vaporization during the drying process of electrode fabrication [32].

Fig. 2 shows the EDX spectra of GO (A), MWCNT (B), GO-MWCNT (C) and ERGO-MWCNT (D) modified films. All the modified films contain almost same proportion of carbon content while variation in the oxygen proportion which find a way to monitor the formation of composite. EDX profile of GO exhibited oxygen weight % of 45.66, attributed to the presence of oxygen functionalities (hydroxyl, epoxy and carboxyl groups) on the surface of graphene sheets and also indicating versatile oxidation has been achieved. On the other hand, EDX profile of MWCNT exhibits carbon wt. % of 88.85 and oxygen wt. % of 11.15. Here, the presence of oxygen content might be caused by the moisture adsorbed on the film of MWCNT modified film. Interestingly, EDX profile of GO-MWCNT exhibits carbon wt. % of 70.65 and oxygen wt. % of 29.35. A significant increase in the oxygen wt. % has been achieved comparing with pristine MWCNT and GO-MWCNT. The increased oxygen content of GO-MWCNT is due to the association of GO with MWCNT, which gives evidence for the composite formation. EDX profile of GO-MWCNT exhibits carbon wt. % of 84.87 and oxygen wt. % of 15.13. When, comparing the EDX profile of GO-MWCNT (C) and ERGO-MWCNT(D), a considerable decrease in oxygen wt. % was observed from 29.35 to 15.13, revealing the substantial reduction of oxygen functionalities through the electrochemical reduction. Thus, EDX spectra confirming the formation of ERGO-MWCNT formation by comparing the carbon and oxygen wt. %.

3.2. Electrochemical characterization of the anode

Fig. 3A shows the cyclic voltammograms (CVs) obtained at ERGO (a), MWCNT (b), ERGO-MWCNT (c) ERGO-MWCNT/GOx/Nf film modified GCEs in N₂ saturated 0.1M PBS at the scan rate of 50mVs⁻¹. In the absence of GOx, no redox peaks were obtained for ERGO, MWCNT [33], ERGO-MWCNT modified films, whereas well defined sharp redox peak has been obtained when GOx was immobilized onto the ERGO-MWCNT modified GCE. The redox couple have a formal potential (E^o) of -0.430 with a low peak to peak separation value (ΔE_p) of 29 mV. Evidently the redox peak obtained for ERGO-MWCNT/GOx/Nf is ascribed to the direct electrochemistry of GOx (FAD/FADH₂) at the ERGO-MWCNT modified film. Besides, the low ΔE_p value achieved on the composite modified electrode shows that GOx is highly immobilized onto the modified film which accelerates the electron transfer between the active sites of enzyme and electrode surface. The probable reason for the efficient electron shuttling behavior of ERGO-MWCNT is the synergistic effect of ERGO and MWCNT. Since, both ERGO and MWCNT have large surface area and high conductivity, the combination of both as

composite could harvest all the excellent properties of the two carbon materials. Hence the composite exhibits combined large surface area which assists more enzyme loading and leads to the direct electrochemistry of GOx. Moreover, the high conductivity of the composite directs the enhanced peak currents than the pristine MWCNT or ERGO.

Fig. 3B shows the cyclic voltammograms obtained at ERGO-MWCNT/GOx/Nf composite film modified GCE in deoxygenated PBS of pH 7 at different scan rates. The redox peak currents linearly increased with the scan rates from 10 to 100 mVs^{-1} (Inset to Fig. 3B), indicating a surface-controlled process.

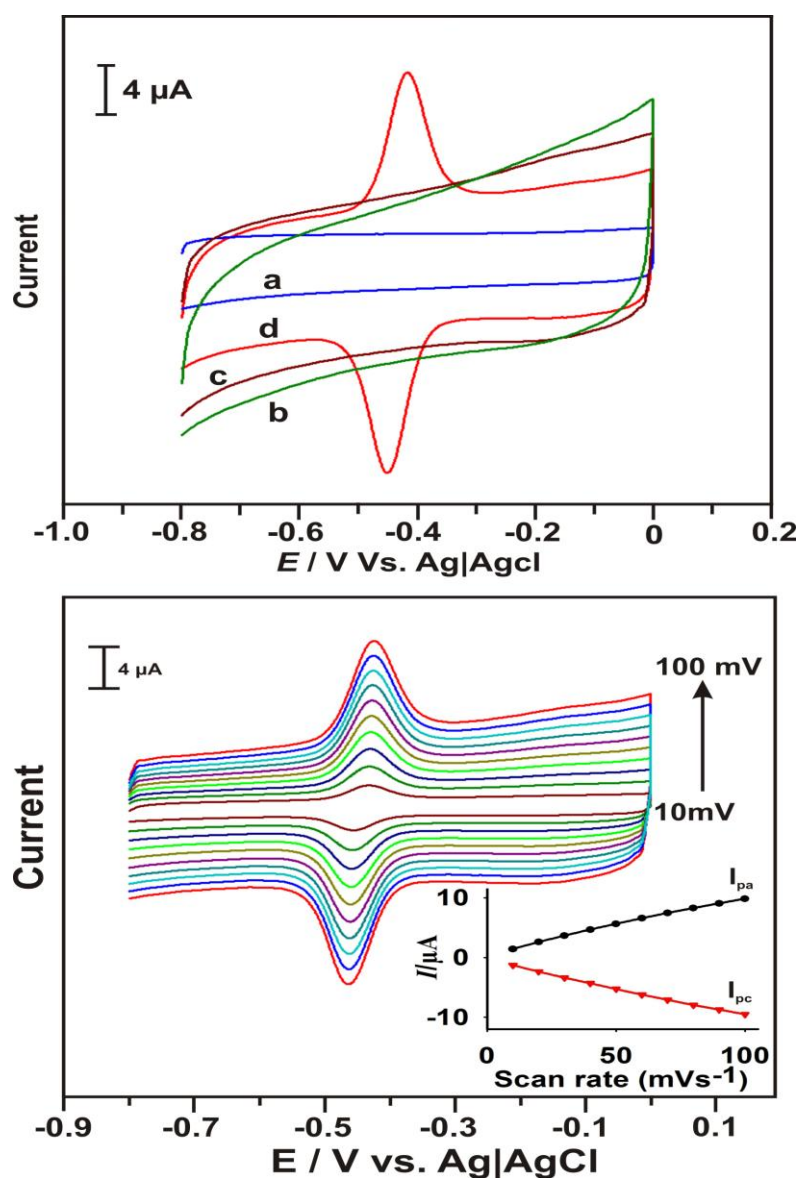


Figure 3. (A) CVs obtained at ERGO (a), MWCNT (b), ERGO-MWCNT (c) ERGO-MWCNT/GOx/Nf film modified GCEs in N_2 saturated 0.1M PBS at the scan rate of 50mVs^{-1} . (B) CVs of ERGO-MWCNT/GOx/Nf film modified GCE at various scan rates (from inner to outer: 10, 20, 30, 40, 50, 60, 70, 80, 90 and 100mVs^{-1}). Inset is the plot of scan rate versus I_{pa} and I_{pc} .

3.3 Electrocatalysis towards glucose in the presence of HQ

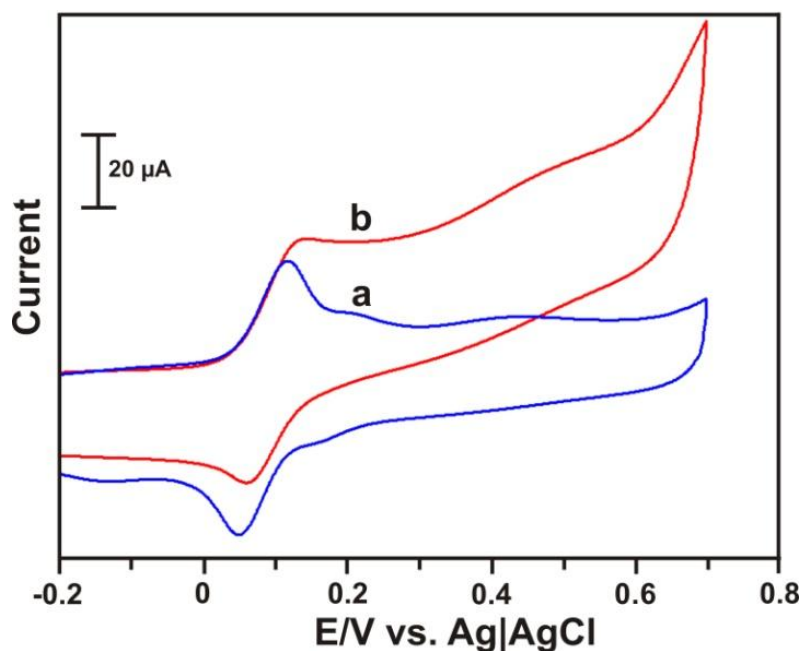


Figure 4. CVs of ERGO-MWCNT/GOx/Nf modified GCE in N_2 saturated PBS (pH 7) containing 0.5 mM Hydroquinone in the absence of glucose (a) and presence of 10 mM glucose (b) at the scan rate of 50 mVs^{-1} .

Fig. 4 shows the CVs of ERGO-MWCNT/GOx/Nf modified GCE in N_2 saturated 0.1M PBS (pH 7) containing 0.5 mM Hydroquinone in the absence of glucose (a) and presence of 10 mM glucose with the scan rate of 50 mVs^{-1} . Cyclic voltammograms of ERGO-MWCNT/GOx/Nf modified GCE exhibited characteristic well defined redox peaks of hydroquinone in the absence of glucose. This redox peaks are the characteristic redox reaction of HQ centered at approximately 0.08 V [12, 34]. The anodic current begins to increase from more negative potential, which has significant advantages for the biofuel cell applications [35, 36]. Since, more negative potential will increase the cell voltage, which obviously increase the output current of the biofuel cell. Thus, the ERGO-MWCNT/GOx/Nf modified GCE exhibited efficient and enhanced electrocatalytic ability towards mediated electro-oxidation of glucose in the presence of mediator HQ.

3.4 Surface morphological characterization of cathode

The SEM image of the graphene shows the typical wrinkled and folded morphology of the graphene sheets (Fig. 5A). Fig. 5B depicts the SEM image of the prepared graphene – Pt composite. It portrays that Pt nanoparticles were spread widely and randomly over the entire surface of the graphene sheets with nanoparticles size in the range of few nanometers. The morphology results confirmed the formation of graphene and graphene- Pt composite. Further this morphology is essential for the high surface area of the composite and ultimately provides more active sites for the electrocatalysis of oxygen reduction.

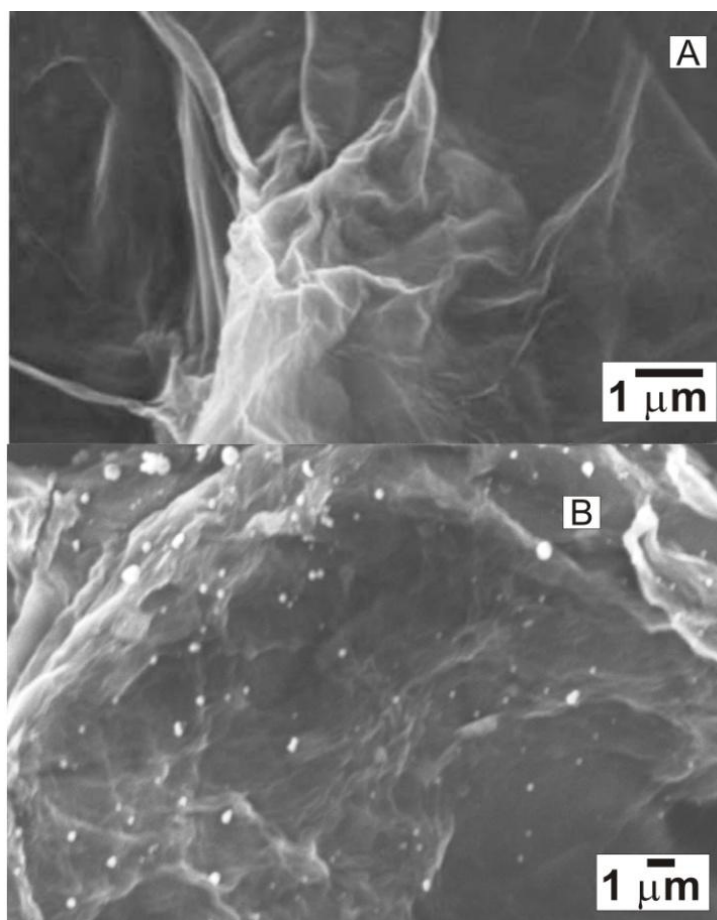


Figure 5. SEM images of graphene (A) and graphene – Pt composite films (B).

3.5 Electrocatalytic oxygen reduction at the graphene-Pt composite modified GCE

Fig. 6A shows the cyclic voltammograms of Graphene-Pt composite modified GCE in N_2 saturated (a), ambient air (b) and oxygen saturated (c) 0.1 M phosphate buffer of pH 7 at the scan rate of 50 mVs^{-1} . Under ambient air condition, the graphene-Pt composite exhibits increased cathodic current, compared with that of nitrogen saturated condition. On the other hand, the modified electrode displays highly enhanced sharp cathodic current occurring at $\sim 0.062 \text{ V}$ (onset potential ~ 0.4) under oxygen saturated PBS. This could be ascribed to the excellent electrocatalytic reduction of O_2 at the graphene-Pt modified electrode. The results prove that graphene is a versatile platform to stabilize the platinum nanoparticles. Fig. 6B shows the linear sweep voltammograms (LSVs) of Graphene-Pt composite modified GCE in N_2 saturated (a), ambient air (b) and oxygen saturated (c) 0.1 M phosphate buffer of pH 7 at the scan rate of 50 mVs^{-1} . The cathodic peak current obtained at ambient air condition is more than that of under N_2 saturated PBS. Whereas, under oxygen saturated condition graphene- Pt modified GCE shows greatly enhanced cathodic current centered at $\sim 0.062 \text{ V}$ coinciding with the results obtained by cyclic voltammetry. Thus both CV and LSV studies demonstrated that graphene-Pt composite have excellent electrocatalytic ability towards O_2 reduction and this could be attributed to the synergy of high surface area of graphene and outstanding electrocatalytic ability of platinum nanoparticle.

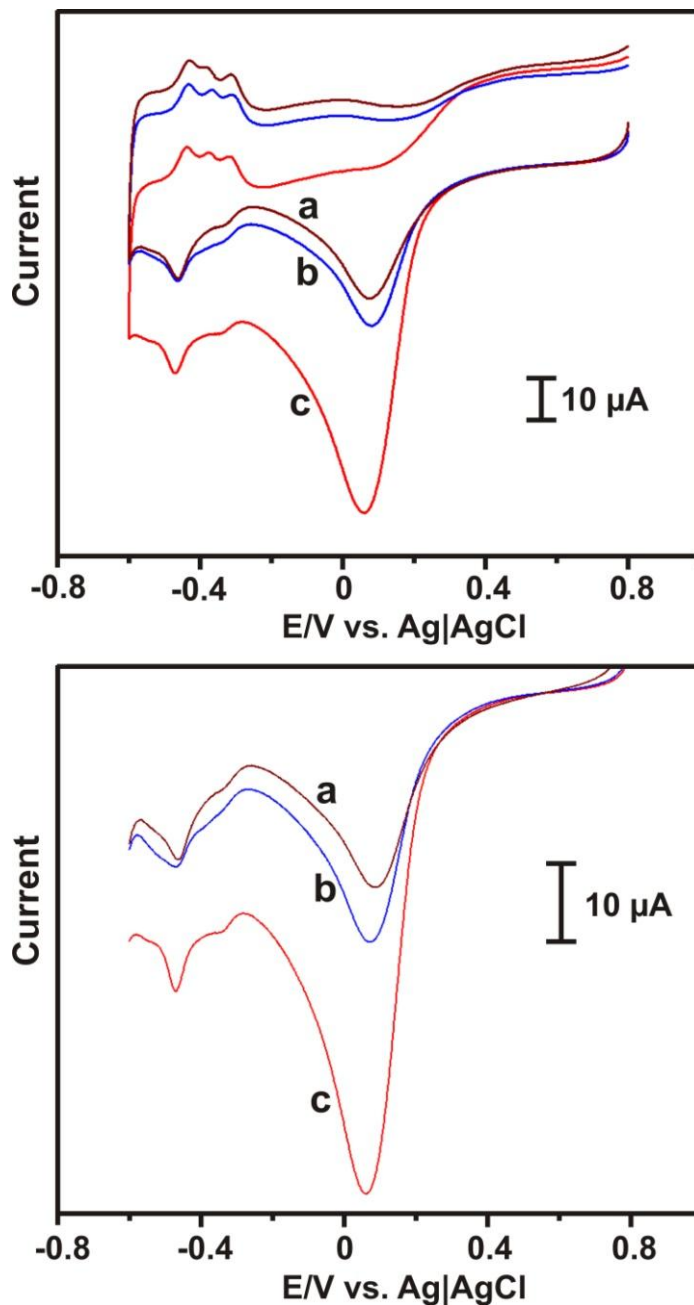


Figure 6. (A) CVs of Graphene-Pt composite modified GCE in N₂ saturated (a), ambient air (b) and oxygen saturated (c) 0.1 M PBS (pH 7) at the scan rate of 50 mVs⁻¹. (B) LSVs of Graphene-Pt composite modified GCE in N₂ saturated (a), ambient air (b) and oxygen saturated (c) 0.1 M PBS (pH 7) at the scan rate of 50 mVs⁻¹.

3.6 Biofuel cell construction and performance

A membraneless biofuel cell has been composed by assembling ERGO-MWCNT/GO_x/Nf modified GCE (anode) and graphene-Pt composite film modified GCE (cathode) together as shown in scheme 1. The electrolyte is physiological buffer (0.1 M PBS of pH 7) for the both anode and cathode. 10 mM concentration of glucose in 0.1 M PBS (of pH 7) containing 0.5 mM of HQ has been employed

for the anode compartment; while O_2 saturated PBS was employed for the cathode compartment. Polarization and performance curves of the assembled biofuel cell have been given in Fig. 7.

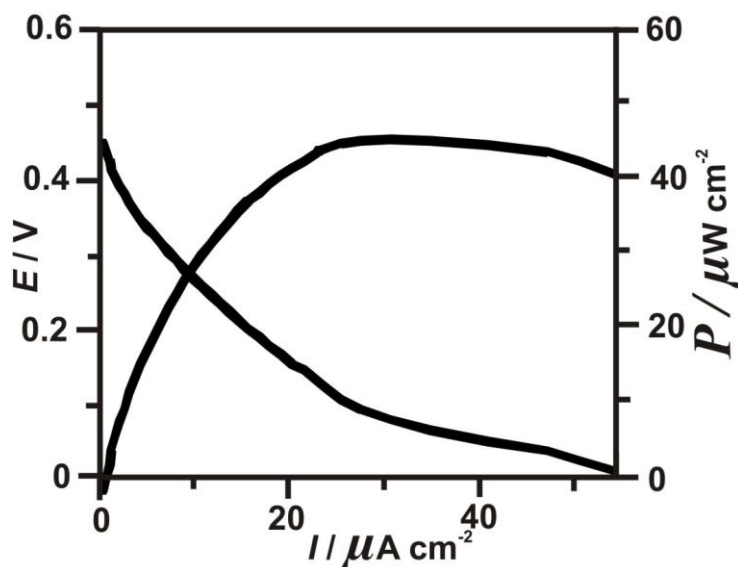


Figure 7. Polarization and performance curves of the constructed biofuel cell with GO-MWCNT/GOx/Nf modified GCE as anode and graphene-Pt modified GCE as a cathode in the presence of 10 mM glucose.

The open circuit voltage (V_{OC}) of the biofuel cell is approximately 0.4 V and maximum power density of $46 \mu W cm^{-2}$ has been achieved. Further, research is under way to improve the power density of the assembled glucose/ O_2 biofuel cell. The above results demonstrate that ERGO-MWCNT composite and graphene-Pt composite to be versatile platform for the development of other kinds of biofuel cell.

4. CONCLUSIONS

We demonstrated a membraneless glucose/ O_2 biofuel cell with GOx immobilized ERGO-MWCNT as the anode for the glucose oxidation and graphene-Pt nanocomposite as the cathode for the O_2 reduction. The anode exhibits excellent catalytic ability towards glucose in the presence of redox mediator hydroquinone (HQ), whereas cathode exhibits exceptional catalytic ability towards oxygen reduction. The results showed that graphene based composites are potential candidates for the development of efficient biofuel cells. Further research is underway in our lab to fabricate a glucose biosensor with ERGO-MWCNT composite modified electrode.

ACKNOWLEDGEMENT

This work was supported by the National Science Council and the Ministry of Education of Taiwan (Republic of China).

References

1. X. Li, L. Zhang, L. Su, T.Ohsaka, L. Mao, *Fuel Cells*, 9 (2009) 85.
2. A.T. Yahiro, S.M. Lee, F.O. Kimble, *Biochim. Biophys. Acta*, 88 (1964) 375.
3. S.C. Barton, J. Gallaway, P. Atanassov, *Chem. Rev.*, 104 (2004) 4867.
4. J. Sun, Y. Hu, Z. Bi, Y. Cao, *J. Power Sources*, 187 (2009) 471.
5. M. Zhou, N. Zhou, F. Kuralay, J.R. Windmiller, S. Parkhomovsky, G.V.-Ramirez, E. Katz, J. Wang, *Angew. Chem. Int. Ed.*, 51 (2012) 2686.
6. M. Zhou, F. Kuralay, J.R. Windmiller, J. Wang, *Chem. Commun.*, 48 (2012) 3815.
7. A. Zebda, L. Renaud, M. Cretin, C. Innocent, R. Ferrigno, S. Tingry, *Sens. Actuators, B*, 149 (2010) 44.
8. H. Sakai, T. Nakagawa, Y. Tokita, T. Hatazawa, T. Ikeda, S. Tsujimura, K. Kano, *Energy Environ. Sci.*, 2 (2009) 133..
9. R.A. Bullen, T.C. Arnot, J.B. Lakemanc, F.C. Walsh, *Biosens. Bioelectron.*, 21 (2006) 2015.
10. J. Kim, J. Parkey, C.Rhodes, A.G.- Martin, *J. Solid State Electrochem.*, 13 (2009) 1043.
11. J. Shim, G.-Y. Kim, S.-H. Moon, *J. Electroanal. Chem.*, 653 (2011) 14.
12. Y. Li, S.-M. Chen, R.Sarawathi, *Int. J. Electrochem. Sci.*, 6 (2011) 3776.
13. X. Wang, D. Li, T. Watanabe, Y. Shigemori, T. Mikawa, T. Okajima, L. Mao, T. Ohsaka, *Int. J. Electrochem. Sci.*, 7 (2012) 1071.
14. X. Sun, Y. Xu, J. Wang, S. Mao, *Int. J. Electrochem. Sci.*, 7 (2012) 3205.
15. Y.-J. Chang, A. P. Periasamy, S.-M. Chen, *Int. J. Electrochem. Sci.*, 6 (2011) 4188.
16. M.-Y. Yen, M.-C. Hsiao, S.-H. Liao, P.-I Liu, H.-M. Tsai, C.-C.M. Ma, N.-W. Pu, M.-D. Ger, *Carbon*, 49 (2011) 3597.
17. Y. Yan, W. Zheng, L. Su, L. Mao, *Adv. Mater.*, 18 (2006) 2639.
18. Y. Liu, S. Dong, *Electrochem. Commun.*, 9 (2007) 1423.
19. S.C. Wang, F. Yang, M. Silva, A. Zarow, Y. Wang, Z. Iqbal, *Electrochem. Commun.*, 11 (2009) 34.
20. S.W. Ting, A.P. Periasamy, S.-M. Chen, R. Saraswathi, *Int. J. Electrochem. Sci.*, 6 (2011) 4438.
21. X. Li, H. Song, Y. Zhang, H. Wang, K. Du, H. Li, Y. Yuan, J. Huang, *Int. J. Electrochem. Sci.*, 7 (2012) 5163.
22. T.-H. Tsai, S.-C. Chiou, S.-M. Chen, *Int. J. Electrochem. Sci.*, 6 (2011) 3333.
23. V. Mani, A.P. Periasamy, S.-M. Chen, *Electrochem. Commun.*, 17 (2012) 75.
24. W. Zheng, H.Y. Zhao, J.X. Zhang, H.M. Zhou, X.X. Xu, Y.F. Zheng, Y.B. Wang, Y. Cheng, B.Z. Jang, *Electrochem. Commun.*, 12 (2010) 869.
25. C.Liu, Z. Chen, C.-Z. Li, *IEEE Trans. nanotechnol.*, 10 (2011) 59.
26. C. Liu, S. Alwarappan, Z. Chen, X. Kong, C.-Z. Li, *Biosens. Bioelectron.*, 25 (2010) 1829.
27. C. Zhang, L. Ren, X. Wang, T. Liu, *J. Phys. Chem. C*, 114 (2010) 11435.
28. L. Qiu, X. Yang, X. Gou, W. Yang, Z.F. Ma, G.G. Wallace, D. Li, *Chem. Eur. J.*, 16 (2010) 10653.
29. H.L. Guo, X.F. Wang, Q.Y. Qian, F.B. Wang, X.H. Xia, *ACS Nano*, 3 (2009) 2653.
30. Y. Li, L. Tang, J. Li, *Electrochem. Commun.*, 11 (2009) 846.
31. W.S. Hummers, R.E. Offeman, *J. Am. Chem. Soc.*, 80 (1958) 1339.
32. H. Tang, J. Chen, S. Yao, L. Nie, G. Deng, Y. Kuang, *Anal. Biochem.*, 331 (2004) 89.
33. K.C. Lin, T.H. Tsai, S.M. Chen, *Biosensors and Bioelectronics*, 26 (2010) 608.
34. A. Chaubey, B.D. Malhotra, *Biosens. Bioelectron.* 17 (2002) 441.
35. T. Tamaki, T. Ito, T. Yamaguchi, *J. Phys. Chem. B*, 111 (2007) 10312.
36. X.-Y. Yang, G. Tian, N. Jiang, B.-L. Su, *Energy Environ. Sci.*, 5 (2012) 5540.